Advanced Composite Materials
Publication details, including instructions for authors and subscription information:
http://www.tandfonline.com/loi/tacm20

Modeling a creep behavior of cross-ply laminates with progressive transverse cracking

Keiji Ogi [a] & Yoshihiro Takao [b]
[a] School of Mechanical and Materials Engineering, University of Surrey, Guildford, Surrey GU2 5XH, UK
[b] Research Institute for Applied Mechanics, Kyushu University, 6-1 Kasuga-Koen, Kasuga, Fukuoka, 816-8580, Japan
Version of record first published: 02 Apr 2012.

To cite this article: Keiji Ogi & Yoshihiro Takao (1999): Modeling a creep behavior of cross-ply laminates with progressive transverse cracking, Advanced Composite Materials, 8:2, 189-203

To link to this article: http://dx.doi.org/10.1163/156855199X00191

Adv. Composite Mater., Vol. 8, No. 2, pp. 189–203 (1999)

Modeling a creep behavior of cross-ply laminates with progressive transverse cracking

KEIJI OGI [1,*] and YOSHIHIRO TAKAO [2]

[1] *School of Mechanical and Materials Engineering, University of Surrey, Guildford, Surrey GU2 5XH, UK*

[2] *Research Institute for Applied Mechanics, Kyushu University, 6-1 Kasuga-Koen, Kasuga, Fukuoka, 816-8580, Japan*

Received 14 July 1998; accepted 11 August 1998

Abstract—A creep model is established for a cross-ply laminate in which the transverse crack density is increasing. Viscoelasticity theory and shear lag analysis are employed for this creep model and the transverse crack density is expressed as a function of both time and stress, based on a probabilistic failure model. The creep compliance of the cross-ply laminate is determined from creep tests of $[90°_8]$ specimens. The creep strain and transverse crack density of $[0/90°_3]_S$ cross-ply laminates are measured during the creep tests and predicted creep strains using the present model agree well with the experimental ones.

Keywords: Transverse crack; creep; cross-ply; viscoelasticity; shear lag model.

1. INTRODUCTION

Mechanical behavior under various environments should be characterized for the use of fiber reinforced composites in engineering fields. Because polymer matrix composites show time-dependent behavior intrinsically, characterization of the long-term behavior of those materials is essential. In addition to viscoelastic deformation, damage, such as transverse cracking and delamination, is expected to increase with time under creep loading in composite laminates.

Creep behavior in composites materials has been studied mostly by using a viscoelasticity or viscoplasticity theory. Lou and Shapery [1] established a nonlinear viscoelasticity constitutive equation based on the thermodynamic theory. Horoschenkoff [2] applied Shapery's theory to the tensile creep behavior of $[90°_8]$ and $[\pm 45°_4]_S$ carbon/epoxy and carbon/PEEK laminates. Dillard *et al.* [3] and Dillard and Brinson [4] employed a nonlinear compliance model based on the Findley

*To whom correspondence should be addressed. E-mail: k.ogi@surrey.ac.uk

power law to describe the viscoelastic response in composite laminates. Flaggs and Crossman [5] developed a constitutive model on the basis of a linear viscoelasticity theory. Chung *et al.* [6] proposed a viscoplasticity model by means of a one-parameter creep potential function.

Development of transverse cracking in cross-ply laminates has been investigated so far by employing a shear lag analysis and a statistical approach. Manders *et al.* [7] investigated multiple fracture in glass/epoxy cross-ply laminates on the basis of a Weibull distribution of the failure strain. Fukunaga *et al.* [8] predicted the transverse crack density using a shear lag model and statistical strength analysis. Peters [9] discussed the strength of 90° plies in cross-ply laminates based on the Weibull strength distribution. Lim and Hong [10] proposed a modified shear lag model, which satisfied more refined boundary conditions.

In contrast, transverse cracking behavior during creep loading has not been discussed well analytically in the previous work, though an experimental investigation has been conducted by Moore and Dillard [11].

In the present paper, transverse cracking in a cross-ply laminate under creep loading is discussed. First, a creep model is developed to predict the strain under constant stress based on viscoelasticity theory and shear lag analysis. The transverse crack density is given as a function of both time and stress using the stochastic failure concept. The strain increments due to both viscoelastic deformation and transverse cracking are taken into account in the model. Secondly, creep tests for $[90°_8]$ and $[0/90°_3]_s$ specimens are carried out at a constant stress and temperature to measure the strains. The change in the transverse crack density in the $[0/90°_3]_s$ specimens are obtained as a function of time during the creep tests. Finally, the predicted strains are compared with the experimental ones to verify the present model.

2. CREEP MODEL

2.1. Creep strain of an intact laminate

The strain response to a given time history of stresses $\boldsymbol{\sigma}(t)$ in a composite lamina is expressed by using the hereditary integral as

$$\boldsymbol{\varepsilon}(t) = \boldsymbol{S}(t)\boldsymbol{\sigma}(0) + \int_{0^+}^{t} \boldsymbol{S}(t-\tau)\frac{\mathrm{d}\boldsymbol{\sigma}(\tau)}{\mathrm{d}\tau}\,\mathrm{d}\tau, \tag{1}$$

where $\boldsymbol{S}(t)$ is the creep compliance matrix of a lamina. By the transformation of the coordinate system, equation (1) leads to

$$\overline{\boldsymbol{\varepsilon}}(t) = \overline{\boldsymbol{S}}(t)\overline{\boldsymbol{\sigma}}(0) + \int_{0^+}^{t} \overline{\boldsymbol{S}}(t-\tau)\frac{\mathrm{d}\overline{\boldsymbol{\sigma}}(\tau)}{\mathrm{d}\tau}\,\mathrm{d}\tau. \tag{2}$$

A bar denotes a property with respect to the off-axis coordinate system. The Laplace transformation of equation (2) yields

$$\hat{\bar{\boldsymbol{\varepsilon}}}(s) = s\hat{\bar{\boldsymbol{S}}}(s)\hat{\bar{\boldsymbol{\sigma}}}(s), \tag{3}$$

where a circumflex accent denotes the Laplace transform. Similarly, the following stress–strain relation is obtained:

$$\hat{\bar{\boldsymbol{\sigma}}}(s) = s\hat{\bar{\boldsymbol{Q}}}(s)\hat{\bar{\boldsymbol{\varepsilon}}}(s), \tag{4}$$

where $\hat{\bar{\boldsymbol{Q}}}(s)$ is the Laplace transform of an off-axis relaxation modulus matrix.

We consider a balanced symmetric laminate which consists of n sheets of laminae with an identical thickness h/n and which is subjected to in-plane loading. The force resultant vector of the laminate is expressed as

$$\boldsymbol{N}(t) = \int_{-h/2}^{h/2} \bar{\boldsymbol{\sigma}}(t)\,\mathrm{d}z = \frac{h}{n}\sum_{k=1}^{n} \bar{\boldsymbol{\sigma}}^{(k)}(t). \tag{5}$$

The superscript k stands for the k-th lamina in the laminate. Using equations (4) and (5) we obtain the strain vector of the laminate as

$$\boldsymbol{\varepsilon}(t) = L^{-1}\left[\frac{s}{h}\hat{\boldsymbol{J}}(s)\hat{\boldsymbol{N}}(s)\right], \tag{6}$$

where $L^{-1}[f(t)]$ stands for the inverse Laplace transform of a function $f(t)$ and $\hat{\boldsymbol{J}}(s)$ denotes the Laplace transform of the creep compliance matrix expressed as

$$\hat{\boldsymbol{J}}(s) = \frac{n}{s^2}\left\{\sum_{k=1}^{n} \hat{\bar{\boldsymbol{Q}}}^{(k)}(s)\right\}^{-1}. \tag{7}$$

Under a uniaxial constant stress σ_x, equation (6) yields

$$\boldsymbol{\varepsilon}(t) = \sigma_x \boldsymbol{J}(t)\boldsymbol{e}_1, \tag{8}$$

where $\boldsymbol{e}_1$ is a unit vector of $(1, 0, 0,)^t$.

2.2. Creep strain of a cross-ply laminate with transverse cracking

In order to obtain the strain and stress distributions in a cross-ply laminate with transverse cracking, a modified shear lag model [8, 10] shown in Fig. 1 is employed in the present analysis (see Appendix). It is assumed that all the elastic moduli are functions of time while they are independent of the stress state, and that the residual thermal strains are independent of time. Figure 2 shows a schematic drawing of the crack spacing and corresponding strain as functions of time. The crack spacing is constant ($2L_k$) during $t_k \leqslant t < t_{k+1}$. Creep strain increment $\Delta\boldsymbol{\varepsilon}_k^C$ is generated during this time span. At the moment of $t = t_{k+1}$, the crack

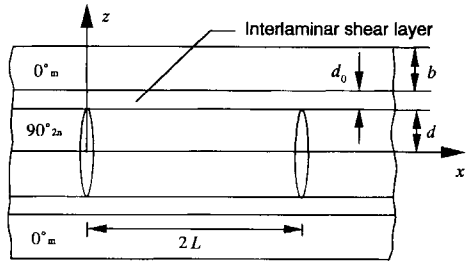

Figure 1. A modified shear lag model with transverse cracks [8].

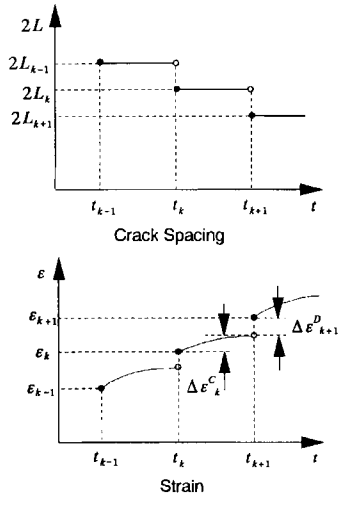

Figure 2. Change in the transverse crack density and strain with time in the present model.

spacing suddenly changes to $2L_{k+1}$, which causes the increase in the average strain by $\Delta\boldsymbol{\varepsilon}^D_{k+1}$. Accordingly, the strain $\boldsymbol{\varepsilon}_{k+1}$ of a 0°-ply at $t = t_{k+1}$ is expressed as

$$\boldsymbol{\varepsilon}_{k+1} = \boldsymbol{\varepsilon}_k + \Delta\boldsymbol{\varepsilon}^C_k + \Delta\boldsymbol{\varepsilon}^D_{k+1}, \tag{9}$$

with $\boldsymbol{\varepsilon}_k$ of the strain for $t = t_k$. The average creep strain of the 0°-ply at $0 \leqslant x \leqslant L_k$ is given by

$$\boldsymbol{\varepsilon}^{(1)C}(t) = \frac{1}{L_k}\int_0^{L_k} \boldsymbol{\varepsilon}^{(1)C}(t, x)\,\mathrm{d}x - \boldsymbol{\varepsilon}^{(1)T}, \tag{10}$$

where $\boldsymbol{\varepsilon}^{(1)T}$ and $\boldsymbol{\varepsilon}^{(1)C}(t, x)$ denote the residual thermal strain and the creep strain of the 0°-ply at t and x, respectively. The latter strain is expressed by using a hereditary integral as

$$\boldsymbol{\varepsilon}^{(1)C}(t, x) = \boldsymbol{S}^{(1)}(t)\boldsymbol{\sigma}^{(1)}(0, x) + \int_0^t \boldsymbol{S}^{(1)}(t-\tau)\frac{\mathrm{d}\boldsymbol{\sigma}^{(1)}(\tau, x)}{\mathrm{d}\tau}\,\mathrm{d}\tau, \tag{11}$$

where $\boldsymbol{S}^{(1)}(t)$ is the creep compliance of the 0°-ply without any cracks and $\boldsymbol{\sigma}^{(1)}(t, x)$ is the stress distribution in the 0°-ply. Using the above shear lag model the strain distribution in the 0°-ply is expressed by

$$\boldsymbol{\varepsilon}^{(1)^C}(t, x) = \boldsymbol{\varepsilon}^0(t) + \boldsymbol{\varepsilon}^{(1)^T} + \boldsymbol{K}_1(t) f(x), \tag{12}$$

with

$$\boldsymbol{K}_1(t) = L^{-1}\left[s^2 \hat{\boldsymbol{S}}^{(1)}(s)\, \hat{\boldsymbol{Q}}^A(s) \hat{\boldsymbol{\varepsilon}}^0(s) + s \hat{\boldsymbol{S}}^{(1)}(s)\, \hat{\boldsymbol{Q}}^A(s) \boldsymbol{\varepsilon}^{(2)^T}\right], \tag{13}$$

$$\boldsymbol{Q}^A(t) = \frac{d}{b}\begin{bmatrix} Q_{22}(t) & Q_{12}(t) \\ \dfrac{Q_{12}Q_{22}}{Q_{11}}(t) & \dfrac{Q_{12}}{Q_{11}}(t) \end{bmatrix}, \tag{14}$$

where b and d denote half thickness of the 0°- and 90°-ply, respectively, $\boldsymbol{\varepsilon}^0(t)$ is the uniform mechanical strain of an intact laminate, and $\boldsymbol{\varepsilon}^{(2)^T}$ is the residual thermal strain of the 90°-ply. Then, substitution of equation (12) into equation (10) leads to the average creep strain of the laminate as

$$\boldsymbol{\varepsilon}^{(1)^C}(t) = \boldsymbol{\varepsilon}^0(t) + \boldsymbol{K}_1(t) \frac{\tanh(L_k\alpha)}{L_k\alpha}, \tag{15}$$

where α is a shear lag parameter (see Appendix). When the crack spacing changes from $2L_k$ to $2L_{k+1}$ at $t = t_{k+1}$, the average strain increment due to cracking is expressed as

$$\Delta\boldsymbol{\varepsilon}^D_{k+1} = \left\{\frac{\tanh(L_{k+1}\alpha)}{L_{k+1}\alpha} - \frac{\tanh(L_k\alpha)}{L_k\alpha}\right\}\boldsymbol{K}_2(t_{k+1}), \tag{16}$$

with

$$\boldsymbol{K}_2(t) = \left\{\frac{d}{b}\frac{\sigma^{(2)}_{x0}(t)}{Q_{11}(t)}, 0\right\}^t, \tag{17}$$

where $\sigma^{(2)}_{x0}(t)$ is a uniform stress of the 90°-ply composed of the mechanical and thermal stresses. Thus, the strain at an arbitrary time during $t_n \leqslant t < t_{n+1}$ is obtained as

$$\boldsymbol{\varepsilon}(t) = \boldsymbol{\varepsilon}^0(t) + \boldsymbol{K}_1(t)\frac{\tanh(L_n\alpha)}{L_n\alpha} + \sum_{k=1}^{n}\left[\left\{\boldsymbol{K}_2(t_k) - \boldsymbol{K}_1(t_k)\right\}\left\{\frac{\tanh(L_k\alpha)}{L_k\alpha} - \frac{\tanh(L_{k-1}\alpha)}{L_{k-1}\alpha}\right\}\right], \tag{18}$$

which needs the creep compliance $\boldsymbol{S}^{(1)}(t)$ and the crack spacing as functions of time. Summation of the first and second terms gives a creep strain of a laminate with the crack spacing $2L_n$. When no creep deformation occurs during each time span, the function $\boldsymbol{K}_1(t)$ is identical to $\boldsymbol{K}_2(t)$ and the third term vanishes. If the

crack spacing is constant even if creep deformation occurs, the third term equals zero, too. Therefore, the third term represents the interference effect between creep deformation and progressive transverse cracking.

Here we assume the following creep compliance and relaxation modulus matrices

$$\boldsymbol{S}^{(1)}(t) = \begin{bmatrix} S_{11}^0 & S_{12}^0 \\ S_{12}^0 & S_{22}^0 + p_{22}(1 - \mathrm{e}^{-t/T'}) \end{bmatrix}, \tag{19}$$

$$\boldsymbol{Q}^{(1)}(t) = \begin{bmatrix} Q_{11}^0 & Q_{12}^0 - q_{12}(1 - \mathrm{e}^{-t/T}) \\ Q_{12}^0 - q_{12}(1 - \mathrm{e}^{-t/T}) & Q_{22}^0 - q_{22}(1 - \mathrm{e}^{-t/T}) \end{bmatrix}, \tag{20}$$

where S_{ij}^0 and Q_{ij}^0 are the initial values of each component, and p_{22}, q_{22} and q_{12} are constants. When $S_{22}(t)$ is given as a function of time, the relaxation modulus $\boldsymbol{Q}^{(1)}(t)$ is obtained using the following equations:

$$q_{22} = \frac{p_{22}Q_{22}^0}{1 + p_{22}Q_{22}^0}, \quad q_{12} = -\frac{S_{12}^0}{S_{11}^0}p_{22}, \tag{21}$$

$$e^{-t/T'} = \frac{Q_{22}^0 \mathrm{e}^{-t/T}}{Q_{22}^0 - q_{22}(1 - \mathrm{e}^{-t/T})}. \tag{22}$$

Then, we can neglect the interference term in the longitudinal direction by assuming the following equations:

$$K_{1x}(t) = K_{2x}(t) = \frac{d}{b}\frac{\sigma_{x0}^{(2)}(t)}{Q_{11}^0} \equiv K_x(t). \tag{23}$$

Strictly speaking, the strain increases discontinuously with time as shown in Fig. 2 because progressive transverse cracking occurs at random of time. However, the continuous increase in the strain can be assumed if the crack density is given as a continuous function of time. Therefore, the longitudinal strain at an arbitrary time is derived from equations (8), (18) and (23) as

$$\varepsilon_x(t, \sigma) = J_{11}(t)\sigma + K_x(t)\frac{2\rho(t, \sigma)}{\alpha}\tanh\frac{\alpha}{2\rho(t, \sigma)}, \tag{24}$$

where $\rho(t, \sigma)$ is the crack density which is the inverse of $2L$.

2.3. Transverse crack density under creep loading

Based on the stochastic theory, the crack density is assumed as

$$\rho(t, \sigma) = [1 - R(t, \sigma)]\{\rho_s - \rho_0(\sigma)\} + \rho_0(\sigma), \tag{25}$$

where $\rho_0(\sigma)$, ρ_s, and $R(t, \sigma)$ are the initial crack density, saturation crack density, and reliability probability function, respectively. The initial crack density is

expressed in a form of the Weibull distribution as [7]

$$\rho_0(\sigma) = \{1 - \exp(-A\sigma^l)\}\rho_s, \tag{26}$$

where parameters A and l are constants. Next, modifying Coleman's theory [12], the reliability probability function is expressed as

$$R(t, \sigma) = \exp\left[-\Psi\left[\int_0^t \phi[\sigma(t)]\,dt\right]\right], \tag{27}$$

with

$$\Psi(x) = \alpha x^p, \quad \phi(\sigma) = \beta\sigma^q, \tag{28}$$

in which parameters α, β, p, and q are constants. In the case of a creep test, equation (27) is rewritten as

$$R(t, \sigma) = \exp(-B\sigma^m t^n), \tag{29}$$

where parameters B, m, and n are empirically determined constants. Substituting equations (26) and (29) into equation (25), the crack density is described as

$$\rho(t, \sigma) = \left[1 - \exp(-A\sigma^l - B\sigma^m t^n)\right]\rho_s. \tag{30}$$

It should be noted that $\rho(0, \sigma) = \rho_0(\sigma)$ is obtained from this equation. Equation (30) can be rewritten as

$$\ln\left(\ln\left(\frac{\rho_s - \rho_0}{\rho_s - \rho(t, \sigma)}\right)\right) = \ln B\sigma^m + n \ln t. \tag{31}$$

The procedure for determining the parameters A, B, l, m, and n is as follows. The parameters A and l are determined from the plots of the crack density as a function of stress in monotonic tensile tests. Next, by plotting the left-hand term of equation (31) against $\ln t$ for two different stresses, the parameters B, m, and n are obtained.

3. EXPERIMENTAL

Coupon specimens of $[90°_8]$ and $[0/90°_3]_s$ CF/epoxy laminates (T800H/#3631, Toray) were fabricated for monotonic and creep tests. The thickness of all the specimens is about 1.1 mm and the width is 20 mm and 8 mm for $[90°_8]$ and $[0/90°_3]_s$, respectively. Strain gages with the gage length of 30 mm were adhesively bonded to the specimens under the condition of a temperature of 110°C for two hours to avoid hardening of the adhesive layer during the creep tests. Monotonic tensile tests were conducted for $[0/90°_3]_s$ specimens at a temperature of 110°C to obtain the crack density as a function of applied stress. Creep tests of $[90°_8]$ and $[0/90°_3]_s$ specimens were also conducted at the same temperature to measure the change in the strain with time. The creep compliance and relaxation modulus were

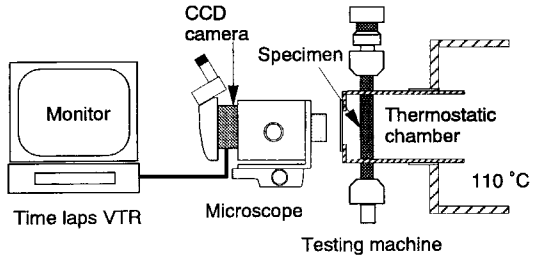

Figure 3. Experimental set-up for *in-situ* observation of transverse cracking during a creep test at a high temperature.

expressed in the form of equations (19) and (20), respectively, using the creep test results of $[90°_8]$ specimens. Figure 3 shows an experimental setup for the monotonic and creep tests. An electrohydraulic testing machine was used together with a thermostatic chamber for tests. Transverse cracking in $[0/90°_3]_s$ specimens during the creep tests was monitored *in-situ* by a stereoscopic microscope and recorded by a VTR through a CCD camera. Transverse crack density was measured within the range of 30 mm length corresponding to the gage length of the strain gage and was defined as the number of cracks per unit centimeter.

4. RESULTS AND DISCUSSION

Figure 4 shows the change in the creep compliance $S_{22}(t)$ obtained from a $[90°_8]$ specimen under creep loading. The initial stress of 45 MPa (strain of 0.68%) was selected because the time to failure is too short to measure the creep compliance at a higher stress. Obvious creep deformation is observed only at less than 5000 s. Table 1 shows the elastic constants and parameters in equations (19) and (20) at a temperature of 110°C. Figure 5 shows the typical results of change in the strain of a $[0/90°_3]_s$ specimen during a creep test. Abrupt increases in the strain correspond to transverse cracking within the gage section of the strain gage. Predicted strains using the measured crack density and equation (18) are also shown in Fig. 5. A shear lag parameter α is determined from the amount of the increase in the strain due to transverse cracking. Agreement between the experimental and predicted ones is fairly good.

Figure 6 shows a tip of a transverse crack using an optical microscope and a C-scan view after a creep test at a stress of 530 MPa. Any remarkable delamination from transverse crack tips is not observed, although transverse cracks with a small opening displacement are not detected in the C-scan view because the frequency of an acoustic lens (30 MHz) is low. Figure 7 shows the change in the crack density with time for ten $[0/90°_3]_s$ specimens at various stresses. Final failure occurs in some specimens in which high stresses are applied when the crack

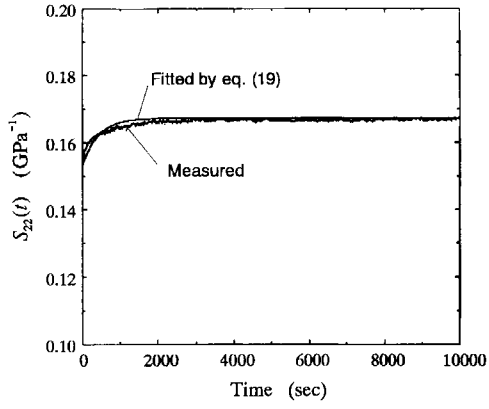

Figure 4. Creep compliance $S_{22}(t)$ obtained from a $[90°_8]$ specimen at a stress of 45 MPa and temperature of 110°C.

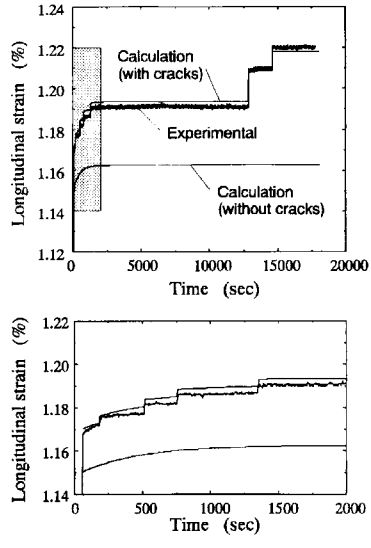

Figure 5. Measured and predicted (equation (18)) creep strains in a $[0/90°_3]_S$ specimen at a stress of 510 MPa. The hatched region in the upper figure is enlarged into the lower one.

Table 1.
Material properties in equations (19) and (20)

S^0_{11} (GPa^{-1})	6.58×10^{-3}	S^0_{12} (GPa^{-1})	-2.35×10^{-3}	S^0_{22} (GPa^{-1})	0.153
Q^0_{11} (GPa)	153	Q^0_{12} (GPa)	2.34	Q^0_{22} (GPa)	6.56
p_{22} (GPa^{-1})	0.0139	q_{12} (GPa)	0.195	q_{22} (GPa)	0.546
T' (s)	421	T (s)	419		

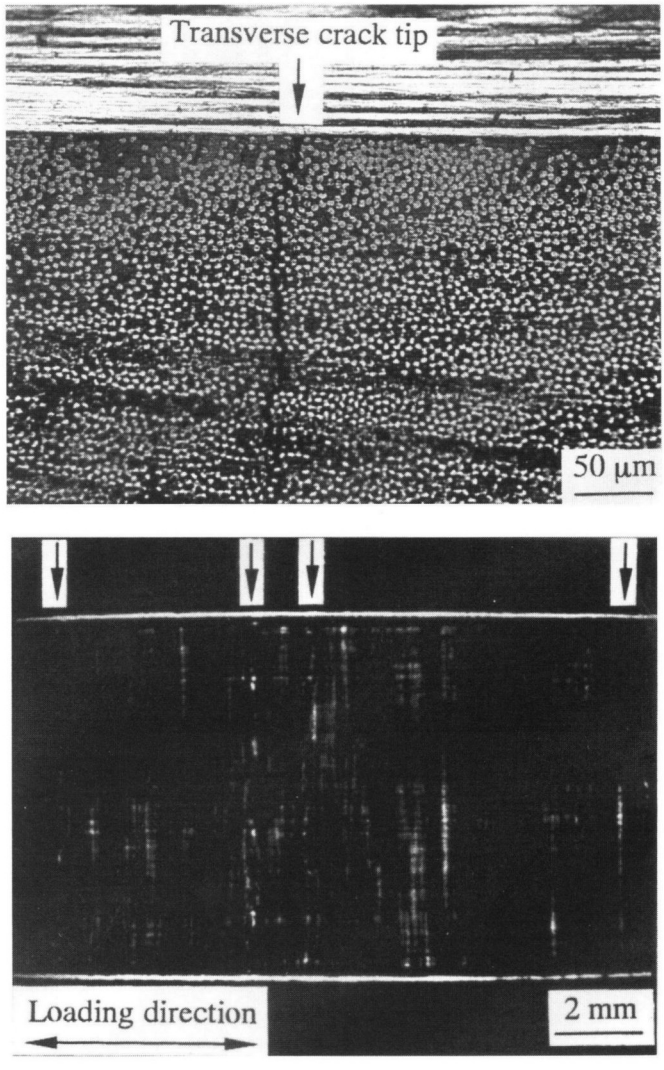

Figure 6. An edge view of a transverse crack tip (upper) and a C-scan view (lower) of a $[0/90^\circ_3]_S$ specimen after a creep test at a stress of 510 MPa. Arrows in the lower photo show the positions of transverse cracks which are not detected by C-scan.

density approaches a saturation value (6/cm). There are two different stages for the evolution of transverse cracking. The crack density increases gradually as the creep strain increases in the first stage of $0 < t < 5000$ s. Most of the transverse cracks in this stage are generated by the increase in the strain due to viscoelastic deformation. In the second stage of $t > 5000$ s, the crack density continues to increase although the increase in the creep strain is very small. Transverse cracking in the latter could be classified as the delayed fracture.

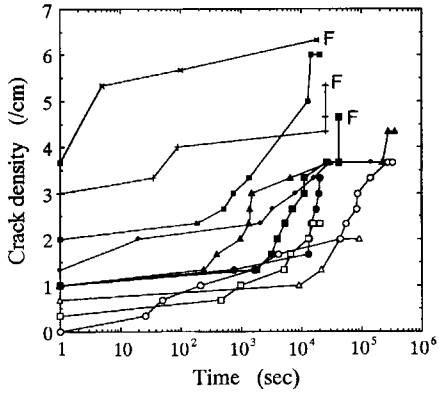

Figure 7. Change in the transverse crack density with time during the creep tests of ten $[0/90°_3]_S$ specimens at various stresses. The symbol F means that final failure occurs during the creep test.

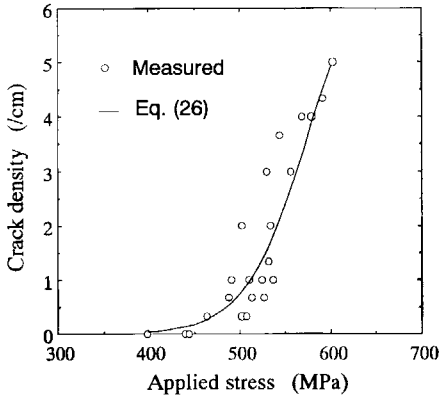

Figure 8. Change in the transverse crack density as a function of applied stress in the monotonic tensile tests of $[0/90°_3]_S$ specimens.

Figure 8 shows the crack density as a function of applied stress from the monotonic tensile tests of $[0/90°_3]_S$ specimens. Since most of the specimens were broken before the transverse crack density was saturated, the saturation crack density was determined from the creep tests. Using Figure 8, the parameters A and l in equation (26) are determined. On the other hand, the parameters B, m, and n are determined from the plots of equation (31) for stresses of 500 and 530 MPa. Almost the same values of n are obtained for both stresses. Figure 9 presents the measured and predicted (equation (30)) crack density against time at a stress of 530 MPa. The values of the parameters in equation (30) are summarized in Table 2.

Figure 10 shows the comparison of the strains in a $[0/90°_3]_S$ specimen during creep loading between the experimental and predicted (equation (24)) results. The

Table 2.
The parameters in equation (30)

ρ_S (/cm)	6.0	l	14.0
A (GPa^{-l})	2230	m	12.9
B (GPa^{-m} s^{-n})	157	n	0.267

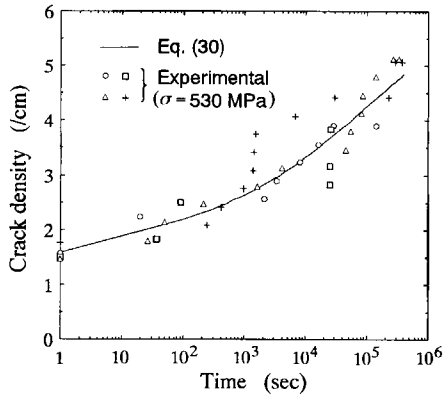

Figure 9. Measured and predicted crack density against time during the creep tests of four $[0/90°_3]_S$ specimens at a stress of 530 MPa.

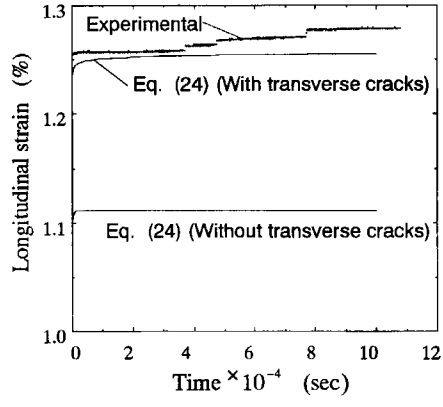

Figure 10. Comparison of the strains in a $[0/90°_3]_S$ specimen during a creep test at a stress of 530 MPa between the experimental and predicted results.

predicted ones increase continuously because a continuous increase in the crack density (equation (30)) is employed. Good agreement between them is obtained. For more precise prediction, transverse crack density should be measured by a strain gage with longer gage length at various stresses.

5. CONCLUSIONS

A creep model of a cross-ply laminate with transverse cracking is proposed using the viscoelasticity theory, shear lag analysis and probabilistic failure model. Longitudinal strains are obtained as equations (18) and (24) by assuming discontinuous and continuous increase in the transverse crack density, respectively. It is proved that transverse cracking occurs both during and after the remarkable viscoelastic deformation. Strains predicted by equations (18) or (24) agree well with the experimental results of the creep tests of the cross-ply laminates. Practically, equation (24) is sufficiently useful.

Acknowledgements

The present research was supported in part by grant-in-aid (No. 09751009) for Scientific Research of the Ministry of Education, Science, Sports and Culture of Japan.

REFERENCES

1. Y. C. Lou and R. A. Shapery, Viscoelastic characterization of a nonlinear fiber-reinforced plastic, *J. Compos. Mater.* **5**, 208–234 (1971).
2. A. Horoschenkoff, Characterization of the creep compliances J_{22} and J_{66} of orthotropic composites with PEEK and epoxy matrices using the nonlinear viscoelastic response of the neat resins, *J. Compos. Mater.* **24**, 879–891 (1990).
3. D. A. Dillard, D. H. Morris and H. F. Brinson, Predicting viscoelastic response and delayed failures in general laminated composites, in: *Composite Materials: Testing and Design (Sixth Conference), ASTM STP 787*, I. M. Daniel (Ed.), pp. 357–370. American Society of Testing and Materials, Philadelphia (1982).
4. D. A. Dillard and H. F. Brinson, A numerical method for predicting creep and delayed failures in laminated composites, in: *Long-term Behavior of Composites, ASTM STP 813*, T. K. O'Brien (Ed.), pp. 23–37. American Society of Testing and Materials, Philadelphia (1983).
5. D. L. Flaggs and F. W. Crossman, Analysis of the viscoelastic response of composite laminates during hygrothermal exposure, *J. Compos. Mater.* **15**, 21–40 (1981).
6. I. Chung, C. T. Sun and I. Y. Chang, Modeling creep in thermoplastic composites, *J. Compos. Mater.* **27**, 1009–1029 (1993).
7. P. W. Manders, T.-W. Chou, F. R. Jones and J. W. Rock, Statistical analysis of multiple fracture in 0°/90°/0° glass fibre/epoxy resin laminates, *J. Mater. Sci.* **18**, 2876–2889 (1983).
8. H. Fukunaga, T.-W. Chou, P. W. M. Peters and K. Schulte, Probabilistic failure strength analysis of graphite/epoxy cross-ply laminates, *J. Compos. Mater.* **18**, 339–356 (1984).
9. P. W. M. Peters, The strength distribution of 90° plies in 0/90/0 graphite-epoxy laminates, *J. Compos. Mater.* **18**, 545–556 (1984).
10. G. Lim and C. S. Hong, Prediction of transverse cracking and stiffness reduction in cross-ply laminated composites, *J. Compos. Mater.* **23**, 695–713 (1989).
11. R. H. Moore and D. A. Dillard, Time-dependent matrix cracking in cross-ply laminates, *Compos. Sci. Technol.* **39**, 1–12 (1990).
12. B. D. Coleman, On the strength of classical fibers and fiber bundles, *J. Mech. Phys. Solids* **7**, 60–70 (1958).

APPENDIX: THE MODIFIED SHEAR LAG ANALYSIS [8, 10]

Introducing the interlaminar shear layers and taking into account the thermal residual stresses, the strain distributions in 0°-ply and 90°-ply are expressed as

$$\begin{aligned}
\varepsilon_x^{(1)} &= \varepsilon_{x0}^{(1)} + \frac{d\sigma_{x0}^{(2)}}{bQ_{11}} f(x), \\
\varepsilon_x^{(2)} &= \varepsilon_{x0}^{(2)} - \frac{\sigma_{x0}^{(2)}}{Q_{22}} f(x), \\
\varepsilon_y^{(1)} &= \varepsilon_{y0}^{(1)}, \\
\varepsilon_y^{(2)} &= \varepsilon_{y0}^{(2)}, \\
\gamma_{xy}^{(1)} &= \gamma_{xy}^{(2)} = 0,
\end{aligned} \tag{A1}$$

with

$$\begin{aligned}
&\varepsilon_{x0}^{(1)} = \varepsilon_x^0 + \varepsilon_x^{(1)^T}, \quad \varepsilon_{x0}^{(2)} = \varepsilon_x^0 + \varepsilon_x^{(2)^T}, \\
&\varepsilon_{y0}^{(1)} = -\nu\varepsilon_x^0 + \varepsilon_y^{(1)^T}, \quad \varepsilon_{y0}^{(2)} = -\nu\varepsilon_x^0 + \varepsilon_y^{(2)^T}, \\
&f(x) = \frac{1 - e^{-2\alpha L}}{e^{2\alpha L} - e^{-2\alpha L}} e^{\alpha x} + \frac{e^{2\alpha L} - 1}{e^{2\alpha L} - e^{-2\alpha L}} e^{-\alpha x}, \\
&\alpha = \sqrt{\frac{G}{d_0}\left(\frac{1}{bQ_{11}} + \frac{1}{dQ_{22}}\right)}.
\end{aligned} \tag{A2}$$

The superscripts 1 and 2 denote 0°-ply and 90°-ply, respectively. The uniform strains $\varepsilon_{x0}^{(i)}$, $\varepsilon_{y0}^{(i)}$ $(i = 1, 2)$ are expressed by the summation of the uniform mechanical strain ε_x^0, $-\nu\varepsilon_x^0$ and the residual thermal strain $\varepsilon_x^{(i)^T}$, $\varepsilon_y^{(i)^T}$, respectively, where ν is Poisson's ration of the laminate.

The stress distributions are as follows:

$$\begin{aligned}
\sigma_x^{(1)} &= \sigma_{x0}^{(1)} + \frac{d}{b}\sigma_{x0}^{(2)} f(x), \\
\sigma_y^{(1)} &= \sigma_{y0}^{(1)} + \frac{dQ_{12}}{bQ_{11}}\sigma_{x0}^{(2)} f(x), \\
\sigma_x^{(2)} &= \sigma_{x0}^{(2)}\{1 - f(x)\}, \\
\sigma_y^{(2)} &= \sigma_{y0}^{(2)} - \frac{Q_{12}}{Q_{22}}\sigma_{x0}^{(2)} f(x),
\end{aligned} \tag{A3}$$

where

$$\sigma_{i0}^{(k)} = Q_{ij}\left(\varepsilon_j^0 + \varepsilon_j^{(k)T}\right) \quad (i, j = x, y \text{ and } k = 1, 2). \tag{A4}$$

The uniform stresses $\sigma_{x0}^{(i)}$, $\sigma_{y0}^{(i)}$ consist of the mechanical stress and residual thermal stress, respectively.